Journal of Materials Chemistry C

Accepted Manuscript

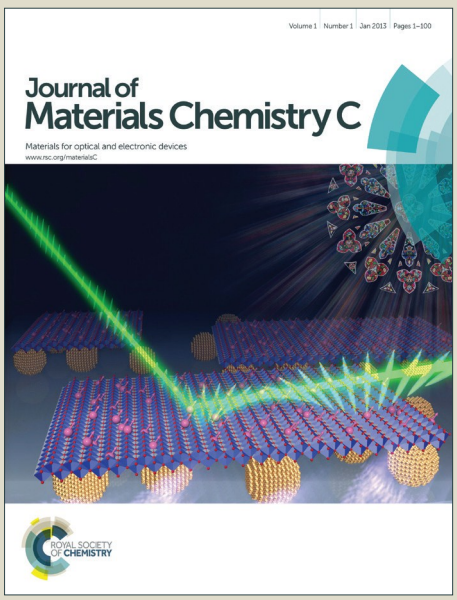

ROYAL SOCIETY OF CHEMISTRY

www.rsc.org/materialsC

Journal of
Materials Chemistry C

ARTICLE

Individual single-crystal nanowires as electrodes for organic single-crystal nanodevices

Received 00th January 20xx,
Accepted 00th January 20xx

DOI: 10.1039/x0xx00000x

www.rsc.org/

Guorui Wang,[a] Qingxin Tang,*[a] Yanhong Tong,*[a] Wenping Hu*[b] and Yichun Liu*[a]

The conductive, transparent, and flexible SnO_2:Sb single-crystal nanowires are shown as electrodes for F_{16}CuPc single-crystal nanowire devices on the flexible plastic which includes anisotropic-transport OFETs, electrode-movable OFETs, and p-n junction photovoltaic devices. The SnO_2:Sb nanowires provide the good energy level match and the excellent soft contact with F_{16}CuPc nanowire, leading to the multifacet applications of the SnO_2:Sb nanowire in nanowire electronics and optoelectronics, and the high device performance. Combined with their good size compatibility these results shows that the conductive SnO_2:Sb single-crystal nanowire opens a window into the fundamental understanding of the intrinsic properties of highly ordered organic semiconductors, optimization and miniaturization of the organic nanocircuits, and development of new-generation flexible organic nanodevice.

Introduction

One ultimate aim of the nanomaterial studies is to achieve the high-performance and low-cost nanocircuits for practice applications in miniaturized electronics and optoelectronics.[1] However, almost all of the reported nanodevices use the macroscopic metal film electrodes, or apply the electron beam lithography/focused ion beam deposition technique to obtain the microscaled electrodes.[2] The former is size incompatible with the ideal nanocircuits. And the latter faces challenge in extension to organic devices due to the fatal irradiation damage of the electrons on the organics.[3] Further, the most commonly used electrode material, Au, has the work function at 5.2 eV. It does not match with numbers of semiconductors, in particular, n-type organic semiconductors, leading to the large parasitic contact resistance with high carrier injection barriers and lack of high-performance n-type organic device.[4]

The Sb doped SnO_2 (SnO_2:Sb) has the low resistivity (10^{-2}-10^{-4} Ωcm) and the high transparency in the visible wavelength range which could transmit most of the sunlight (up to 97%).[5] Its work function is around 4.7-4.9 eV which matches well with the lowest unoccupied molecular orbital (LUMO) level of some of commonly used n-type organic semiconductors, for example, F_{16}CuPc, C_{60}, PTCDI *etc*.[6] Together with its excellent thermal and chemical stabilities, SnO_2:Sb is considered to be one of the most promising candidate as the low-cost electrode for organic electronics/optoelectronics. Here, we applied the high-conductivity, high-transparency, mechanically-flexible SnO_2:Sb single-crystal nanowires as the electrodes, to realize the construction of the organic single-crystal nanodevices on the flexible plastic substrate in air ambience at room temperature, which include the anisotropic-transport F_{16}CuPc nanowire organic field-effect transistors (OFETs), the electrode-movable F_{16}CuPc nanowire OFETs, and the CuPc/F_{16}CuPc nanowire photovoltaic devices. The good size compatibility of the electrode nanowire with the semicoductor nanowire allows higher levels of integration in a given chip area. The nature of the single crystal facilitates revealing the intrinsic transport properties and obtaining the high performance of devices.[3] They also provide the possibility for realization of the optimized complementary symmetry organic nanocircuits, as well as the potential for room-temperature processing and flexible electronics/optoelectronics.

[a] *Key Laboratory of UV Light Emitting Materials and Technology under Ministry of Education, Northeast Normal University, Changchun 130024 (P. R. China)*
E-mail: tangqx@nenu.edu.cn; tongyh@nenu.edu.cn; ycliu@nenu.edu.cn
Fax: +86-431-85099873; Tel: +86-431-85099873
[b] *Beijing National Laboratory for Molecular Sciences, Key Laboratory of Organic Solids, Institute of Chemistry, Chinese Academy of Sciences, Beijing 100190 (P. R. China)*
Email: huwp@iccas.ac.cn
Electronic Supplementary Information (ESI) available: [details of any supplementary information available should be included here]. See DOI: 10.1039/x0xx00000x

Experimental

Single crystal nanowires of F_{16}CuPc, CuPc and SnO_2:Sb were synthesized by physical vapour transport method in a horizontal tube furnace. The F_{16}CuPc, CuPc, and the mixture of Sn and Sb powder, were respectively used as source powder. The bare Si wafers were used as the substrates for the growth of F_{16}CuPc and CuPc nanowires, the 10-nm-Au coated Si wafers was used for the growth of the SnO_2:Sb nanowires. A quartz boat with the source powder was placed at the high-temperature zone, and vaporized at 370-410, 400-500, and 850 °C for F_{16}CuPc, CuPc, and SnO_2:Sb nanowires, respectively. Highly pure Ar was used as the carrier gas, and the system was evacuated by a mechanical pump. The nanowires could be obtained on the substrates located at low temperature. Based on these flexible nanowire, the nanowire devices were fabricated by the mechanical manipulation with the microprobes of a Micromanipulator 6150 probe station with an optical microscope under ambient condition (Fig. S1-S3). The Au film and the individual single-crystal nanowires were successively transferred by a micro mechanical probe. The PMMA in chlorobenzene was spin-coated onto the surface of the flexible substrate (PC, Polycarbonate) as the dielectric. Its thickness can be easily controlled by the spin-coating times, and was measured by an Ambios Technology XP-2 surface profilometer. Dielectric capacitance was calculated using the measured thickness and known dielectric constant of PMMA of 3.9. The field-effect and the photovoltaic properties of the devices were recorded with a Keithley 4200 SCS and the Micromanipulator 6150 probe station in a clean and shielded box at room temperature. SEM images were obtained on a Hitachi S-4300 SE instrument. The mobility was calculated in saturated regime by $I_{SD} = W \cdot \frac{\mu C_i}{L}(V_G - V_T)$, where W is channel width, L is channel length, C_i is dielectric unit area capacitance, and V_T is threshold voltage.

Results and discussion

The single-crystal nanowires as building blocks provide a "bottom-up" paradigm of nanoelectronics. Based on the good flexibility of the SnO_2:Sb nanowires (Fig. S1 and S2, Supporting information), the individual F_{16}CuPc nanowire FETs could be fabricated with the parallel and crossed electrode configuration by a room-temperature mechanical transfer method as shown in Fig. 1a_1-a_2 and 1b_1-b_2. Even, the F_{16}CuPc nanowire could be sandwiched between the two SnO_2:Sb nanowires in the direction of the width of the F_{16}CuPc nanowire (Fig. 2). The size of the electrodes is determined by the dimension of the SnO_2:Sb nanowires. Currently, almost all of the reported organic nanodevices use the macroscopic metal film electrodes. In our devices, the comparable nanowire width of SnO_2:Sb with F_{16}CuPc shows the good size compatibility between the electrode and the active layer, therefore showing the advantage of the SnO_2:Sb nanowire to develop applications in the highly integrated nanowire electronics. Compared with the conventional metal electrode deposition, the mechanical transfer method presented here avoids the thermal irradiation damage on the organic single crystal, and minimizes the leak current between source/drain and gate electrodes due to the absence of the pinhole filling of the high-energy metal atoms.[7]

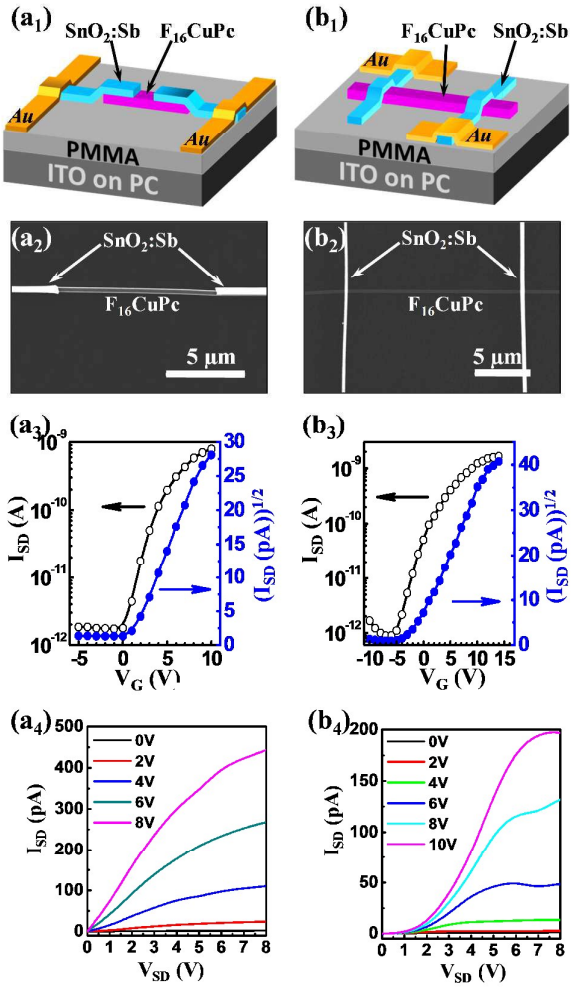

Fig. 1 Schematic images, representive SEM images, representive transfer and output characteristics of F_{16}CuPc nanowire FETs. (a_1-a_4) with parallel nanowire electrodes. For Fig. 1a_3-a_4, the channel length of the device L= 11.6 μm, the channel width W=183 nm (width of the F_{16}CuPc nanowire), the thickness of the dielectric d=750 nm. In Fig. 1a_3, V_{SD}=15 V. (b_1-b_3) with crossed nanowire electrodes. For Fig. 1b_3-b_4, L= 10 μm, W=300 nm, d=650 nm. In Fig. 1b_3, V_{SD}=20 V. All measurements were performed at room temperature in dark.

The versatile FET configuration presented in Fig. 1 and Fig. 2 provides an advantage to study the anisotropic field-effect performance of an individual nanowire. The anisotropic field-effect properties of organic crystals are beneficial for the understanding of the relationship between molecular stacking and charge transport so that direct proofs could be obtained for the further synthesis of high performance organic semiconductors and the fabrication of organic devices.[8-12] Currently, the anisotropic transport of organic crystals mainly focuses on the two-dimensional sheet-like structure regardless of the worldwide study of 1D nanostructures since 1990s. In contrast, it is challenging to study the anisotropy of nanowire,

which requires an electrode gap smaller than the width of nanowire be deposited in the direction of nanowire width. Until now, only Tao's group studied the anisotropic of 4.4'-bis((E)-2(naphthalen-2-yl)vinyl)-1,1'-biphenyl (BNVBP) nanorod FETs by an organic single wire mask method, where a 88.7-nm gap was fabricated in the direction of nanowire width.[13] Here, a new method has been used to investigate the anisotropy transistors of an individual nanowire by sandwiching an individual $F_{16}CuPc$ nanowire between SnO_2:Sb nanowires in both the length and width directions (Fig. 1a and 2). As shown in Fig. 2a-b, the SnO_2:Sb wires are bent against the $F_{16}CuPc$ nanowire and the elasticity of SnO_2:Sb wires provides the additional force perpendicularly to the length direction of $F_{16}CuPc$ nanowire, so that the $F_{16}CuPc$ nanowire can be sandwiched tightly by the two SnO_2:Sb nanowires in the width direction. It should be noted that the fabrication of such a sandwiched device is based on the flexibility and elasticity of the SnO_2:Sb nanowires, which makes the application of the external force becoming feasible during the sandwiching process. Certainly, the flexibility and elasticity of SnO_2:Sb nanowires also depends strongly on their size. It is found that wires with width of 50-300 nm could bend under the touch of the mechanical probes, but would not fracture even when they are bent over 180 degree. Moreover, the bent wires could recover their original morphology after the force from the probes is removed. Oppositely, those wires with width over 300 nm are difficult to be bent by our mechanical probes and easily broken or bounced away when they are bent. Therefore, in our experiments those SnO_2:Sb nanowires with width at ~100-300 nm are selected as the electrodes.

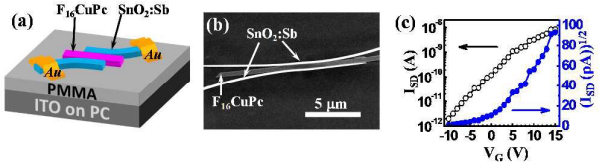

Fig. 2 $F_{16}CuPc$ nanowire FET with sandwiched nanowire electrodes. (a) Schematic image, (b) SEM image, and (c) transfer curves at V_{SD}=10 V. L= 0.5 μm, W=1.2 μm, and d=650 nm.

Representative electrical characteristics of the transistors with three different electrode configurations are shown in Fig. $1a_3$-a_4, $1b_3$-b_4, and 2c. For parallel and crossed devices, the channel width is determined by the width of the $F_{16}CuPc$ nanowire, and the channel length is determined by the length of the $F_{16}CuPc$ nanowire between the SnO_2:Sb nanowire electrodes. For the sandwich device, the channel width is determined by the distance between the contact points of the $F_{16}CuPc$ nanowire and the SnO_2:Sb nanowire electrode, and the channel length is determined by the width of the $F_{16}CuPc$ nanowire (Fig. S4, Supporting information). All of devices exhibit the typical air-stable n-type field-effect characteristics with well-define off state (off-state current I_{off} ~1 pA) and low threshold voltage (< 2V). The mobility of the devices transporting in the width direction of the nanowire is at ~0.0094-0.067 $cm^2V^{-1}s^{-1}$. The highest mobility 0.067 $cm^2V^{-1}s^{-1}$ in the width direction was near one order lower than that of devices with carrier transport along the length direction of the nanowire (0.1-0.5 $cm^2V^{-1}s^{-1}$, Fig. $1a_1$-$1a_3$ and $1b_1$-$1b_3$).

In the process of manipulating the SnO_2:Sb nanowire with the mechanical transfer method, it is found that the excellent flexibility of the SnO_2:Sb nanowire and the weak contact interaction between the SnO_2:Sb nanowire and the substrate allow the SnO_2:Sb nanowire to be multiply taken up and put down (Fig. S2, Supporting information), and even be slid on the substrate surface. Combined with the available electrode configurations of the SnO_2:Sb nanowires (Fig. 1, parallel and crossed configurations), these mechanical properties make it possible to set freely the length of the conducting channel based on one individual $F_{16}CuPc$ single crystal nanowire. Assuming the organic wire as a railway, the SnO_2:Sb nanowire could be "slid" freely on the "railway". As shown in the schematic and SEM images of Fig. 3a and 3b, one end of the $F_{16}CuPc$ nanowire is connected to a parallel SnO_2:Sb nanowire (as the fixed electrode), and the other end is connected across to another SnO_2:Sb nanowire which acts as the "sliding" wire (*i.e.*, as

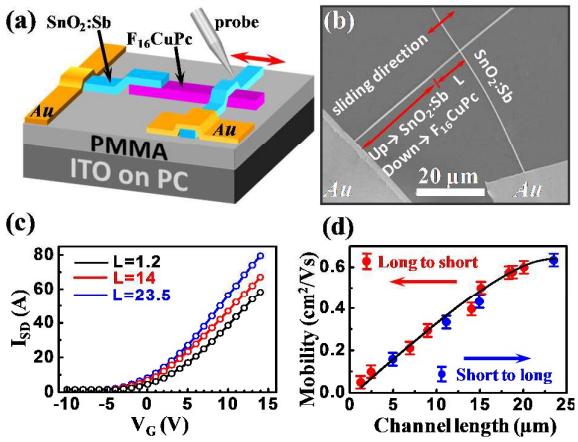

the movable electrode) (Device fabrication process and electrical measurements see Fig. S3a and S5, Supporting information).

Fig. 3 (a-b) Schematic image and representive SEM image of a device with one SnO_2:Sb wire parallel stacking on $F_{16}CuPc$ wire and another SnO_2:Sb crossed stacking on $F_{16}CuPc$ wire, the parallel SnO_2:Sb wire was fixed and the crossed SnO_2:Sb wire could move on the $F_{16}CuPc$ wire to adjust the length of the transistor conducting channel. (c) Representive transfer characteristic of the device with the channel length L=1.21, 14, and 23.5 μm. (d) Mobility dependence of the transistors on the channel length (L) measured by sliding the SnO_2:Sb nanowire from 20 to 1.2 μm, and then from 1.2 to 23.5 μm, the error bars indicate the system error in the channel length measurement (the channel length of the device was measured by SEM and optical microscope, see Fig. S5, Supporting information). V_{SD}=20 V.

Fig. 3c shows the typical transfer characteristic curves of transistors at the different channel lengths of 1.21, 11.1, and 23.5 μm, and Fig. 3d shows the dependence of the mobility on the channel length. For our $F_{16}CuPc$ nanowire devices at different channel lengths, the well-define off state occurs for V_G=-5 V with on/off ratio of over 10^4.

In order to confirm the good repeatability of the experimental data and to ensure the high reliability of the data, the SnO_2:Sb nanowire electrode of the $F_{16}CuPc$ nanowire FET first slid backward with changed channel length from 20 to 1.2 μm (from long to short channel, red dots in Fig. 3d), and then slid forward from 1.2 to 23.5 μm (from short to long channel, blue dots in Fig. 3d). It is found that the dependence of the mobility on the channel length follows the same rule when the SnO_2:Sb nanowire slides forward and backward, as shown in Fig. 3d. The mobility from 0.05 to 0.65 $cm^2V^{-1}s^{-1}$ can be obtained by sliding the SnO_2:Sb nanowire.

The device performance of the single crystal OFETs is strongly dependent on the carrier injection and transport which are determined by many factors including electrode material, electrode contact quality, dielectric material, dielectric/semiconductor contact quality, molecular packing structure, crystal quality, *etc*.[12] In our experiments, it was attractive that $F_{16}CuPc$ exhibited mobility of 0.65 $cm^2V^{-1}s^{-1}$ at the channel length of 23.5 μm. To the best of our knowledge, this value is in a class with the highest mobility for $F_{16}CuPc$ OFETs, and it even surpasses those air-gap $F_{16}CuPc$ nanowire devices with Au film as electrodes.[4,14] The air is believed to be the ideal dielectric for OFETs which eliminates the trapping of carriers in the dielectric and at the interface between the dielectric and semiconductor by eliminating the solid dielectric material.[7,15] Our previously experimental results have confirmed that Au is not an optimized electrode material for $F_{16}CuPc$ transistors due to its mismatch work function (5.2 eV) with $F_{16}CuPc$ (4.8-4.9 eV).[4a] In principle, SnO_2:Sb is preferred as electrode material of $F_{16}CuPc$ transistors than Au because of the smaller energy level mismatch between SnO_2:Sb and $F_{16}CuPc$. Therefore, compared with the air-gap Au-electrode device, the higher mobility of the PMMA-dielectric SnO_2:Sb nanowire-electrode $F_{16}CuPc$ device confirms the good energy level match of SnO_2:Sb with $F_{16}CuPc$. On the other hand, the high mobility also suggests the good interface contact between SnO_2:Sb nanowire and $F_{16}CuPc$ nanowire which mainly benefits from the good flexibility of the SnO_2:Sb nanowires.[16] As shown in Fig. S1 (Supporting Information), the SnO_2:Sb nanowire can be bent over 180° and even folded to form a ring with small radius of curvature. It can also maintain their folded form on the substrate by the van der Waals force.[17] The excellent flexibility of SnO_2:Sb nanowire makes it adjust easily to the shape of the $F_{16}CuPc$ crystal which is favourable for its soft intimate interface contact with the $F_{16}CuPc$ nanowire, resulting in the good field-effect properties of the $F_{16}CuPc$ OFETs based on the SnO_2:Sb nanowire electrodes.

Together with the typical field-effect characteristic and high device performance, the repeatable measurement results shown in Fig. 3d further confirm the good contact of the SnO_2:Sb nanowire into $F_{16}CuPc$ nanowire in the whole process of sliding the nanowire electrode, and that the continuous sliding of the SnO_2:Sb nanowire on the $F_{16}CuPc$ nanowire is non-destructive and reversible, which mainly is attributed to two reasons: first, the weak van der Waals force between SnO_2:Sb nanowire and $F_{16}CuPc$ nanowire facilitates separating easily the SnO_2:Sb nanowire from the initial location of the $F_{16}CuPc$ nanowire, and successfully sliding the electrode nanowire without damaging the organic crystal. Second, the mechanical flexibility of the nanowires ensures the intimate contact between SnO_2:Sb nanowire and $F_{16}CuPc$ nanowire, and between the nanowire and the target substrate/Au film.

Study on the dependence of the channel length on the mobility based on organic crystal gives the ability to modulate the electrical behaviour for future commercial application towards the continuous scaling down of the device dimensions and improved device performance.[18] The single crystal minimizes the detrimental effects of the grains and grain boundaries, and hence gives the possibility to reveal the intrinsic transport properties and shows high device performance.[19] However, the channel length dependent mobility of organic single crystal is rarely studied due to the difficulties in growth of single crystals, fabrication of organic devices, and inconsistency between devices which is caused by contacts, crystal thickness, crystal width *etc*.[18] Bao *et al.* has shown a novel method to investigate the channel length dependent mobility by placing one big rigid bulk crystal on an elastic bottom electrode array patterned with different channel length at the fixed channel width/length ratio.[18a] Here, we applied the movable SnO_2:Sb nanowire electrode to investigate the channel length dependent mobility based on the same $F_{16}CuPc$ nanowire. The flexible nanowire electrode provides the consistent planar contact with the semiconductor active layer (*i.e.*, $F_{16}CuPc$ nanowire). In the measurement process all the device parameters except the channel length, for example, channel width, active layer thickness, active layer quality, interface contact *etc*., would be unchanged. It provides the possibility to present the intrinsic properties of the devices. As shown in Fig. 3d, at the fixed channel width (*i.e.*, the width of the $F_{16}CuPc$ nanowire), the mobility is firstly increased linearly with the increasing of conducting channel, and then saturated gradually. This result is in good agreement with Bao's report on the bulk rubrene crystal at the fixed channel width/length ratio.[18a] In principle, the intrinsic mobility of OFETs is independent on the channel length. The channel resistance $R_{ch}=\rho_{ch}L$, where ρ_{ch} is the channel resistance per unit length and L is the channel length. The apparent mobility can be expressed by $\mu \propto \left[\rho_{ch} + \frac{R_p}{L}\right]^{-1}$, where R_p is parasitic resistance which is related to contact resistance.[20] When the channel is long, $\frac{R_p}{L} \ll \rho_{ch}$ and $\mu \propto \rho_{ch}$, showing the independence of mobility on channel length. When the channel is short, the effect of the parasitic resistance R_p can not be ignored resulting in the increasing mobility with the channel length, as shown in Fig.3d. Even though the good energy match for our SnO_2:Sb nanowire electrode based $F_{16}CuPc$ nanowire device, the effect of the contact barrier on the device performance is still nonnegligible in our devices. With the increase of the channel length, the effect of the parasitic resistance becomes weak. Hence, as shown in Fig. 3d, the mobility presents the saturation trend which suggests 0.65 $cm^2V^{-1}s^{-1}$ is near to the intrinsic mobility in our PMMA dielectric device.

The complementary symmetry circuit is one basic component of the integrated circuits. It requires the field-effect performance as similar as possible for n- and p-type devices, which facilitates decreasing the quiescent current and enhancing the gain with the aim of circuit operation in low power dissipation and high stability. However, the electron mobilities were always 2-3 orders lower than their hole mobilities in most organic devices, resulting in poor symmetry of the organic complementary circuits.[7] Here, the mobility from 0.05 to 0.65 $cm^2V^{-1}s^{-1}$ can be obtained by sliding the SnO_2:Sb nanowire (Fig. 2a). The high and adjustable electron mobility in our devices therefore provides a chance to optimize the complementary symmetry organic nanocircuits.

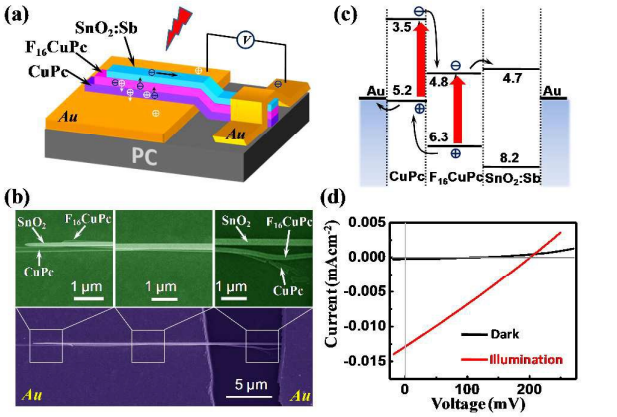

Fig. 4 (a-b) Schematic image and representive SEM images of a Au/CuPc nanowire/F_{16}CuPc nanowire/SnO_2:Sb nanowire photovoltaic device. (c) Band diagram of the device showing the directions of carrier flow. Negative: electron; positive: hole. (d) *I-V* characteristic of the device in dark and under illumination.

From Fig. 3d it is deduced that the mobility should be lower than 10^{-2} $cm^2V^{-1}s^{-1}$ when the channel length is ~500 nm and the carriers transport in the length direction of the F_{16}CuPc nanowire. Compared with that of the devices in the same channel length where the carrier transport in the direction of the width of the F_{16}CuPc nanowire (0.0094-0.067 $cm^2V^{-1}s^{-1}$, Fig. 1c_3), it indicates that the anisotropic transport is almost invisible in our F_{16}CuPc nanowire transistor. It is well known that organic crystals are highly anisotropic,[8] and theoretical and experiment results have confirmed that the electronic coupling is determined by π-stack interaction.[9] Therefore, the highest mobility can be realized in the direction with neighboring molecules in the largest overlap of π molecular orbits. A few research groups have reported the mobility difference at 2-4 times along the different crystalline orientations of the sheet-like organic crystals. For example, Li *et al*. showed the mobility anisotropy of the hexagonal sheet-like thienoacene crystal at 2-2.5.[10] Frisbie reported the mobility of the narrow tetracene sheet along its length direction is 4 times higher than that along its width direction.[11] In theory, the mobility in the direction of the length of the F_{16}CuPc nanowire should be higher than that in the width direction, since the F_{16}CuPc nanowire grows in the strong π-π stacking direction.[4a] As we mentioned above, the apparent mobility is inversely proportional to $\rho_{ch} + \frac{R_p}{L}$. Therefore, the larger contact resistance will decrease the apparent mobility. In our experiments, the electrode interface between SnO_2:Sb nanowire and F_{16}CuPc nanowire is face-contact for the device with sandwiched nanowire electrodes shown in Fig.2, while the electrode interface between one crossed SnO_2:Sb nanowire and the F_{16}CuPc nanowire is point-contact for the device with slidable nanowire electrode shown in Fig.3. The nonlinear output characteristic at low V_{SD} in Fig. 1b_4 suggests the crossed point contact induces the larger contact resistance. Therefore, the mobility in the direction of the nanowire length is decreased. This posssible explains why the anisotropy is invisible in our experiments.

Further, combined with its fully transparency, the SnO_2:Sb nanowires show promising potential as the electrodes of the nanoscaled organic single-crystal solar cells. Very recently, Li et al. report a novel result where organic single-crystalline p-n junction was formed from a mixed solution including p and n materials.[21] In our experiments, the single-crystal nanowire photovoltaic device based on CuPc/F_{16}CuPc p-n junction was fabricated by micro-probe manipulation (Fig. S3b, Supporting information). As shown in Fig. 4a, the CuPc nanowire, the F_{16}CuPc nanowire, and the SnO_2:Sb nanowires were stacked successively on the target substrate with the vertical configuration. The SEM image of the device is given in Fig. 4b. One piece of Au film was pre-attached on the substrate and was connected with one end of the CuPc nanowire. And the other piece of the Au film was overlapped on the end of the SnO_2:Sb nanowire far from the pre-attached Au film. The CuPc nanowire acts as the p-type material and the F_{16}CuPc nanowire services as n-type material of the organic single-crystal nanowire photovoltaic device. The Au film under the CuPc nanowire works as the hole-collecting positive electrode, and the SnO_2:Sb nanowire functions as the transparent negative electrode to collect electrons and to allow the transmission of light. In thin film solar cell, the flow of carriers is limited mainly by scattering events in which carriers have a high instantaneous velocity frequently scatter off lattice vibrations (phonons), defects and impurities.[22] Therefore, the single-crystal nanowire device can effectively enhance the drift velocity of the carriers compared with the commonly used thin film devices. In our experiment, the light is illuminated from the transparent SnO_2:Sb nanowire side, which ensures the light to reach the CuPc/F_{16}CuPc nanowire p-n junction and efficiently generates electron-hole pairs (Fig. 4c), which are then able to flow through an external circuit and provide electrical power. In our experiments, the notable photogenerated voltage and current in the I-V curve in Fig. 4c clearly confirms the excellent contact between the CuPc nanowire/F_{16}CuPc nanowire junction. It further shows that the high quality interface contact between nanowires could be formed by the mechanical probe moving method. Under the illumination of a tungsten bromine lamp with the power of 25 $mWcm^{-2}$, the device yielded a shortcircuit current density (J_{SC}) of ~0.03 $mAcm^{-2}$, an open-circuit voltage (V_{OC}) of ~0.2 V, a fill factor (*FF*) of ~0.26, and an efficiency (η) of ~0.003%. The efficiency is limited mainly by the light absorption efficiency, the junction area, and the thickness of the nanowires. Hence it is possible to further optimize the device performance by apply a sunlight source (the effect of the light source see Fig. S6, Supporting information), combining the wide and narrow band gap organic semiconductors, and selecting the thinner and wider nanowires *etc*.[22]

Conclusions

In conclusion, the SnO_2:Sb single-crystal nanowires as electrodes provide the versatile device configurations for the studies of the anisotropic transport, the channel length dependent mobility, and photovoltaic properties of organic nanowires. The effect of the anisotropic transport on the device performance is found to be almost invisible in the short-channel nanowire FETs. The mobility shows the channel length dependence with firstly linearly increase and gradually

saturation. The notable photogenerated voltage and current can be observed in the CuPc nanowire/F_{16}CuPc nanowire junction. These results show that the SnO_2:Sb single-crystal nanowires as electrode open a window into the fundamental understanding of the intrinsic properties of highly ordered organic semiconductors, optimization and miniaturization of the organic nanocircuits, and development of new-generation flexible organic nanodevices.

Acknowledgements

We are grateful to Prof. Lin Dong (School of Materials Science and Engineering, Zhengzhou University) for pronounced discussion. The authors acknowledge the financial support from National Natural Science Foundation of China (61376074, 51273036, 51322305, 91233204, 61261130092), Ministry of Science and Technology of China (2012CB933703), 111 Project (B13013), China Council Scholarship, and Fundamental Research Funds for the Central Universities (12SSXM001).

Notes and references

1 (a) S. R. A. Raza, S. H. H. Shokouh, Y. T. Lee, R. Ha, H. -J. Choi and S. Im, *J. Mater. Chem. C*, 2014, **2**, 4428; (b) G. A. Salvatore, N. Münzenrieder, T. Kinkeldei, L. Petti, C. Zysset, I. Strebel, L. Büthe and G. Tröster, *Nat. commun.*, 2014, **5**, 2982; (c) S. Kim, A. Konar, W. S. Hwang, J. H. Lee, J. Lee and J. Yang, *Nat. commun.*, 2012, **3**, 1011; (d) H. Li, B. C. K. Tee, G. Giri, J. W. Chung, S. Y. Lee and Z. Bao, *Adv. Mater.*, 2012, **24**, 2588.

2 (a) R. Cheng, S. Jiang, Y. Chen, Y. Liu, N. Weiss, H. C. Cheng, H. Wu, Y. Huang and X. Duan, *Nat. commun.*, 2014, **5**, 5143; (b) H. Li, B. C.-K. Tee, J. J. Cha, Y. Cui, J. W. Chung, S. Y. Lee and Z. Bao, *J. Am. Chem. Soc.*, 2012, **134**, 2760; (c) L. Li, P. Gao, K. C. Schuermann, S. Ostendorp, W. Wang, C. Du, Y. Lei, H. Fuchs, L. D. Cola, K. Müllen and L. Chi, *J. Am. Chem. Soc.*, 2010, **132**, 8807; (d) X. Duan, R. Gao, P. Xie, T. Cohen-Karni, Q. Qing, H. S. Choe, B. Tian, X. Jiang and C. M. Lieber, *Nature Nanotech.*, 2012, **7**, 174.

3 (a) Q. Tang, L. Jiang, Y. Tong, H. Li, Y. Liu, Z. Wang, W. Hu, Y. Liu and D. Zhu, *Adv. Mater.*, 2008, **20**, 2947; (b) Q. Tang, H. Li, M. He, W. Hu, C. Liu, K. Chen, C. Wang, Y. Liu and D. Zhu, *Adv. Mater.*, 2006, **18**, 65.

4 (a) Q. Tang, H. Li, Y. Liu and W. Hu, *J. Am. Chem. Soc.*, 2006, **128**, 14634; (b) J. Zaumseil and H. Sirringhaus, *Chem. Rev.*, 2007, **107**, 1296; (c) L. Li, K. M. -Gresch, L. Jiang, C. Du, W. Wang, H. Fuchs and L. Chi, *Adv. Mater.*, 2012, **24**, 3053.

5 (a) Q. Wan, E. N. Dattoli and W. Lu, *Appl. Phys. Lett.*, 2007, **90**, 222107; (b) L. Li, K. Yu, J. Wu, Y. Wang and Z. Zhu, *Cryst. Res. Technol.*, 2010, **45**, 539.

6 (a) M. Batzill and U. Diebold, *Prog. Surf. Sci.*, 2005, **79**, 47; (b) F. Yang and S. R. Forrest, *Adv. Mater.*, 2006, 18, 2018; (c) H. Dong, H. Zhu, Q. Meng, X. Gong and W. Hu, *Chem. Soc. Rev.*, 2012, **41**, 1754; (d) H. Klauk, *Chem. Soc. Rev.*, 2010, 39, 2643.

7 Q. Tang, Y. Tong, H. Li, Z. Ji, L. Li, W. Hu, Y. Liu and D. Zhu, *Adv. Mater.*, 2008, **20**, 1511.

8 J. Z. V. C. Suandar, V. Podzorov, E. Menard, R. L. Willett, T. Someya, M. E. Gershenson and J. A. Rogers, *Science*, 2004, **303**, 1644.

9 D. A. da Silva Filho, E. G. Kim and J. L. Brédas, *Adv. Mater.*, 2005, **17**, 1072.

10 R. J. Li, L. Jiang, Q. Meng, J. H. Gao, H. X. Li, Q. X. Tang, M. He, W. P. Hu, Y. Q. Liu and D. B. Zhu, *Adv. Mater.*, 2009, **21**, 4492.

11 Y. Xia, V. Kalihari, C. D. Frisbie, N. K. Oh and J. A. Rogers, *Appl. Phys. Lett.*, 2007, **90**, 162106.

12 (a) C. Di, G. Yu, Y. Liu, Y. Guo, Y. Wang, W. Wu and D. Zhu, *Adv. Mater.*, 2008, **20**, 1286; (b) Y. D. Park, J. A. Lim, H. S. Lee and K. Cho, *Mater. Today*, 2007, **10**, 46.

13 T. He, X. Zhang, J. Jia, Yexin Li, and X. Tao, *Adv. Mater.*, 2012, **24**, 2171.

14 (a) Q. Tang, Y. Tong, H. Li and W. Hu, *Appl. Phys. Lett.*, 2008, **92**, 083309; (b) Q. Tang, Y. Tong, H. Li, W. Hu, Q. Wan and T. Bjørnholm, *Adv. Mater.*, 2009, **21**, 4234; (c) Y. Zhang, H. Dong, Q. Tang, Y. He and W. Hu, *J. Mater. Chem.*, 2010, **20**, 7029.

15 E. Menard., V. Podzorov, S. Hur, A. Gaur, M. E. Gershenson, and J. A. Rogers, *Adv. Mater.,* 2004, **16**, 2097.

16 (a) G. S. Tulevski, Q. Miao, A. Afzali, T.O. Graham, C.R. Kagan and C. Nuckolls, *J. Am. Chem. Soc.*, 2006, **128**, 1788; (b) I. H. Campbell, S. Rubin, T. A. Zawodzinski, J. D. Kress, R. L. Martin, D.L. Smith, N. N. Barashkov and J. P. Ferraris, *Phys. Rev. B*, 1996, **54**, R143214; (c) I. H. Cambell, J. D. Kress, R. L. Martin, D. L. Smith, N. N. Barashkov and J. P. Ferraris, *Appl. Phys. Lett.*, 1997, **71**, 3528; (d) J. Wang, H. Wang, J. Zhang, X. Yan and D. Yan, *J. Appl. Phys.*, 2005, **97**, 026106.

17 V. C. Sundar, J. Zaumseil, V. Podzorov, E. Menard, R. L. Willett, T. Someya and M. E. Gershenson, J. A. Rogers, *Science*, 2004, **303**,1644.

18 (a) C. Reese and Z. Bao, *Adv. Funct. Mater.*, 2009, **19**, 763; (b) J. N. Haddock, X. Zhang, S. Zheng, Q. Zhang, S. R. Marder and B. Kippelen, *Org. Electron.*, 2006, **7**, 45.

19 (a) Y. Cao, M. L. Steigerwald, C. Nuckolls and X. Guo, *Adv. Mater.*, 2010, **22**, 20; (b) T. Kobayashi, N. Kimura, J. Chi, S. Hirata and D. Hobara, *Small*, 2010, **6**, 1210; (c) K. A. Singh, T. L. Nelson, J. A. Belot, T. M. young, N. R. Dhumal, T. Kowalewski, R. D. McCullough, P. Nachimuthu, S. Thevuthasan and L. M. Porter, *ACS Appl. Mater. Interfaces*, 2011, **3**, 2973.

20 (a) S. Luan and G. W. Neudeck, *J. Appl. Phys.*, 1992, **72**, 766; (b) M. Leufgen, U. Bass, T. Much, T. Borzenko, G. Schmidt, J. Geurts, V. Wagner and L. W. Molenkamp, *Syn. Met.*, 2004, **146**, 341.

21 H. Li, C. Fan, W. Fu, H. L. Xin, H. Chen, Angew. Chem. Int. Ed. 2015, **54**, 956.

22 A. Kitai, in Principles of solar cells, LED and Diodes: The role of the PN junction, Ch. 1 (Eds. A. Kitai), John Wiley & Sons, Ltd, United Kindom, 2011, **57**.

TOC

The SnO_2:Sb single-crystal nanowires have been shown to function as electrodes to open a window into the fundamental understanding of the intrinsic properties of highly ordered organic semiconductors and the development of the optimized and miniaturized organic nanodevice.